

IV.A.1i Effect of Gaseous Impurities on Durability of Complex Li-based Hydrides for Hydrogen Storage

Dhanesh Chandra (Primary Contact), Joshua Lamb, Wen-Ming Chien, Raja Chellappa*
University of Nevada, Reno (UNR)
MS 388, Chemical and Metallurgical Engineering
Metallurgical and Materials Engineering Division
Reno, NV 89557
Phone: (775) 784-4960; Fax: (775) 784-4316
E-mail: dchandra@unr.edu

* Now at Carnegie Institute of Geophysics, CDAC
Center of Excellence, Washington, D.C.

DOE Technology Development Manager:
Ned Stetson

Phone: (202) 586-9995; Fax: (202) 586-9811
E-mail: Ned.Stetson@ee.doe.gov

DOE Project Officer: Paul Bakke

Phone: (303) 275-4916; Fax: (303) 275-4753
E-mail: Paul.Bakke@go.doe.gov

Contract Number: DE-FC36-05GO15068

Project Start Date: October 1, 2005
Project End Date: September 30, 2010

towards design and synthesis of new hydrogen materials that meet the following DOE 2010 hydrogen storage targets:

- Cost: \$4/kWh net
- Specific energy: 133/kWh/kg
- Energy Density: 2-3 kWh/L

Accomplishments

- Discovered that impurities such as oxygen has greater impact than others such as methane, carbon monoxide or moisture in trace amounts present in hydrogen during pressure cycling of light weight lithium amide-imide complex hydrides (theoretical capacity ~10.5 wt% hydrogen, and ~6 wt% reversible at this time).
- Determined two new phase transitions ($\alpha \rightarrow \alpha' \rightarrow \beta$) in $\text{Ca}(\text{BH}_4)_2$ by in situ neutron diffraction method, details will be released after the acceptance of manuscript submitted.
- Determined $\text{Mg}(\text{BH}_4)_2$ does not contaminate the system by vaporization of the complex hydride itself with no observable vapor contamination from $\text{Mg}(\text{BH}_4)_2$, below 233°C. Above 233°C, partial pressures: $P_{\text{H}_2} = 8.9 \times 10^{-6}$ bar, and $P_{\text{Mg}(\text{BH}_4)_2} = 2.05 \times 10^{-7}$ bar at 255°C.



Objectives

- The overall goal of the entire Hydrogen Storage Program is to develop and verify on-board hydrogen storage systems achieving 2 kWh/kg (6 wt%), 1.5 kWh/L, and \$4/kWh by 2010.
- The specific goal of this project is to understand long-term effects of gaseous impurities on complex metal hydrides, so as to simulate fuel charging from hydrogen gas pumps in vehicular applications.

Technical Barriers

This project addresses the following technical barriers from the Storage section of the Hydrogen, Fuel Cells and Infrastructure Technologies Program Multi-Year research, Development and Demonstration Plan:

- (A) System Weight and Volume
- (D) Durability/Operability

Technical Targets

The project is conducting fundamental and pressure cycling studies on Li amide-imide complex hydrides. Insights gained from these studies will be applied

Introduction

Light-weight complex metal hydrides are becoming increasingly important for hydrogen storage in vehicular applications. Modern hydrogen powered vehicles are expected to be regularly fueled at “hydrogen gas stations.” Research performed on the contemporary hydrides in laboratories generally use ultra-high-purity (UHP) gases that may not reflect on the loading/unloading of the hydride beds that use commercial hydrogen gases. In general, there are trace (ppm) levels of gaseous impurities in commercial hydrogen gas. Complex hydrides generally are composed of reactive metal components, such as Na, Li, K and others, that may readily oxidize even with small amounts of oxygen partial pressure. The degradation of the hydriding properties are generally associated with disproportionation or decomposition of hydride surface or bulk properties of the material during normal periodic charges of impure hydrogen. These studies are expected to lead to the understanding of mechanisms

of degradation, if any, that occur due to repetitive charging of hydrogen in hydride beds. Contamination studies are essential for evaluation of impurity effects, before designing any hydride bed for a vehicular application containing complex hydride materials. Our prior research reflected on degradation testing of the amide-imide complex hydrides, using *industrial grade hydrogen* that contained ppm levels of O_2 , H_2O , N_2 and others which showed *oxygen* contamination was very predominant.

More recently, Mg and Ca hydrides have been investigated for hydrogen storage due their large theoretical ~15% hydrogen capacity with reversible storage capacity of 6.1 wt% hydrogen. The importance of these measurements is that the vaporization behavior of the hydride may be evaluated to check if the original molecular species may be potentially disproportionate subliming undesirable vapors in the system during dehydrating processes. The other borohydride of interest is the $Ca(BH_4)_2$; this material has been prepared by high-pressure methods by Ewa Ronnebro from Sandia National Laboratories using Barkhordarian et al. [1] methodology. Results of cycling/aging of amide-imide, isotherms, and crystal structure analyses are presented. New phase transitions observed in $Ca(BH_4)_2$ hydride are also reported.

Approach

The approach taken is to conduct contamination tests by pressure cycling and aging of materials such as amide-imide hydrogen storage materials, as the primary focus, details of approaches taken are shown in prior annual reports. The specific tasks this year were to determine the changes in the pressure-composition isotherm after cycling with impure hydrogen. A reference temperature of 255°C and a hydrogen pressure range from vacuum to 2 bar was chosen based on the pioneering research of Chen et al. [2]. Typical impurities in commercial hydrogen gas are expected to be O_2 , CO , H_2O , CH_4 , and others minor constituents. As part of collaboration with our Metal Hydride Center of Excellence (MHCoE) members we also performed studies on $Mg(BH_4)_2$ to evaluate impurity contamination from the hydride materials itself due to vaporization and disproportionation using the gravimetric torsion effusion apparatus at UNR. Finally, we performed in situ X-ray diffraction (XRD) studies on $Ca(BH_4)_2$ and observed new phase transformations from the samples synthesized at Sandia National Laboratories; only initial findings are shown in this report with the remainder to be presented later, once the manuscript is accepted. The methodologies developed during this year will be used in the future for new metal hydrides that are being developed by MHCoE partners.

Results

A. Impurity Effects in Imide – Amide System

Extrinsic Pressure Cycling on Li_2NH - $LiNH_2$, with 100 ppm O_2 and H_2O in UHP Hydrogen: We present our extrinsic impurity gas test results after cycling on imide-amide hydrogen storage materials. In addition, we show potential contamination or disproportionation effects due to vaporization magnesium borohydrides.

The hydrogen storage capacity of the Li_3N - Li_2NH - $LiNH_2$ was obtained by volumetric methods. Using Li_3N as starting a material and when we load hydrogen for the time, 10.05 wt% hydrogen is absorbed and forms $LiNH_2$. We show the full spectrum of the isotherm in Figure 1. The crystal structures of these compounds have been described in references [3-7]. Next we show results from cycling experiments in which the starting point of the isotherm is Li_2NH and reversibility is shown between $Li_2NH \leftrightarrow LiNH_2$ absorbing/desorbing approximately 5.6 wt% hydrogen. Details of the cycling procedures have already been presented in other reports. It should be noted that computer program ensures that equilibrium is reached during absorption/desorption cycles until system reaches a prescribed (dp/dt) . The absorption kinetics shows very little change from cycle to cycle, indicating that the capacity losses seen stems largely from a loss in hydrogen capacity of the material.

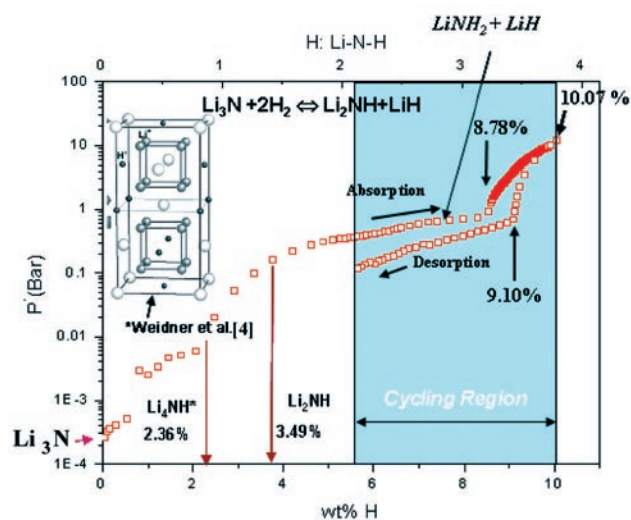


FIGURE 1. Isotherm obtained from hydriding of the precursor α - Li_3N compound is shown indicating theoretical compositions of various compounds. Ideally, the Li_2NH phase absorbs hydrogen from 3.49 to ~10.05 wt% hydrogen. The crystal structures are of each of the phases are listed as follows: 1. α - Li_3N – Hexagonal, P6/mmm - Z = 1 a = 3.6587 Å, c = 3.876 Å, Vol. = 44.933 Å³ [3]. 2. Li_2NH , Tetragonal, I41/a, a = 4.8765(3) Å, c = 9.8769(9) Å, V = 234.9 Å³, Z = 4, Rgt(F) = 0.052, wRref(F2) = 0.121, T = 293 [4,5]. 3. Li_2ND , Cubic – Fm 3m - Z = 4: a = 5.0476 Å, Vol = 128.602 Å³ [6] 4. $LiNH_2$ – BCT, I-4 - Z = 8: a = 5.0695 Å, c = 10.2599 Å, volume = 263.68 Å³ [7]

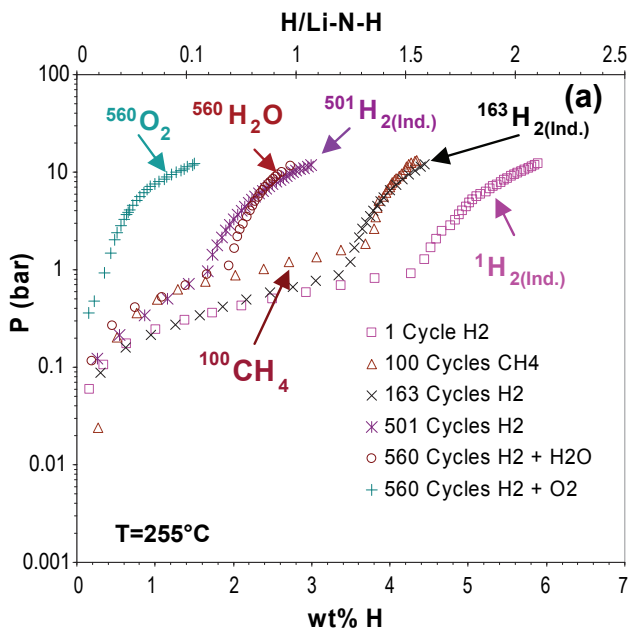


FIGURE 2. Summary of the impurity effects 100 ppm levels of CH_4 , H_2O and O_2 impurities on the cycle life of the lithium amide-imide hydride system. Also included are effects using industrial hydrogen ($\text{O}_2 \sim 10$ ppm, $\text{H}_2\text{O} \sim 32$ ppm, and other low concentration gases).

A summary of the key impurity effect results obtained from pressure cycling of $\text{Li}_2\text{NH} \leftrightarrow \text{LiNH}_2$ are shown in the isotherms obtained at 255°C in Figure 2. Although desorption isotherms for these were obtained, but these are not included for clarity. It should be noted that the isotherms were taken up to 10 bar hydrogen pressure, rather than 20 bar (cycling pressure), for comparison with other data sets that were already obtained. Superscripts on the impurity gas designation on left represent the number of pressure cycles. For

example $^{100}\text{CH}_4$ showed a capacity of 4.2 wt% hydrogen as compared to $^1\text{H}_2$, $^{163}\text{H}_{2\text{indus}}$ of 6.0 wt% and 4.2 wt% hydrogen, respectively. The original capacity is ~ 6.0 wt% hydrogen at 10 bar. For higher number of cycles, as in the case of $^{560}\text{O}_2$ the capacity reduced to ~ 1.5 wt% hydrogen at ~ 10 bar, for $^{560}\text{H}_2\text{O}$ the capacity reduced to 2.7 wt%, as compared to $^{501}\text{H}_{2\text{indus}}$ of 3.01 wt% hydrogen. Experiments with carbon monoxide did not show any measurable loss of hydrogen capacity, data are not shown here. XRD results of the powder obtained in desorbed condition after cycling 100 ppm H_2O added to hydrogen showed the major phases (after desorption) Li_2O , Li_2NH , $\text{Li}(\text{OH})$, and LiH phase. Oxygen, on the other hand, showed a significantly larger capacity loss from cycling compared to similarly cycled impurity gasses. We have also performed impurity testing on mixed hydrides, $3\text{LiNH}_2\text{-Li}_3\text{AlH}_6$ for 540 cycles in 100 ppm O_2 in hydrogen at 325°C , and found only approximately 0.5 wt% loss; performance appeared better than $\text{Li}_2\text{NH-LiNH}_2$ and these data were reported previously. Along with this, it is worth noting that in all cases increased formation of LiH was seen with more cycles observed from XRD results. A portion of the loss in capacity is due to LiH that does not fully transform to Li_2NH each cycle. Table 1 shows the hydrogen capacity with first hydriding from Li_3N phase to LiNH_2 . Table 2 gives a summary of the capacities with different gaseous impurity.

TABLE 1. Overall Hydrogen Capacity of the $\text{Li}_3\text{N-Li}_2\text{NH-LiNH}_2$ Starting from Li_3N Compound

Material	Gas Used	wt% Hydrogen without any cycling from Li_3N precursor
		Number of Cycles = 0
$\text{Li}_2\text{NH-LiNH}_2$	UHP H_2	10.05

TABLE 2. Summary of effects of impurity upon extrinsic pressure cycling. This table includes some of the previous results for comparison. The number in parenthesis represents the number of cycles.

Material	Gas Used	Number of Cycles						
		Temp.(C)	Max. Pr.*	Maximum** wt% absorption of hydrogen as function of number of cycles				
				255	10	1	50- 56	100 to 163
$\text{Li}_2\text{NH-LiNH}_2$	Industrial H_2	255	10	5.8 (1)	4.85 (56)	4.25 (101)	3.05 (501)	3.1 (1,100)
$\text{Li}_2\text{NH-LiNH}_2$	100 ppm O_2 in H_2	255	10	5.8 (1)	-	-	1.45 (560)	-
$\text{Li}_2\text{NH-LiNH}_2$	100 ppm H_2O in H_2	255	10	5.8 (1)	-	-	2.75 (560)	-
$\text{Li}_2\text{NH-LiNH}_2$	100 ppm CH_4 in H_2	255	10			4.88 (100)		
$\text{Li}_2\text{NH-LiNH}_2$	100 ppm CO in H_2	325	12	6.3 (1)				

* Approximate maximum pressure (bar) of isotherm at which the wt% values are reported.

** The hydrogen absorption capacities are reported after the first cycle by normalizing the data to Li_2NH as starting point. The maximum observed reversible capacity is approximately 5.6 wt% between $\text{Li}_2\text{NH} \leftrightarrow \text{LiNH}_2$, although 6.3 wt% is observed during absorption of the very first loading. Note that the Li_2NH does not completely reverse to Li_2NH or Li_3N which yield a hydrogen capacity of 10.07 wt%.

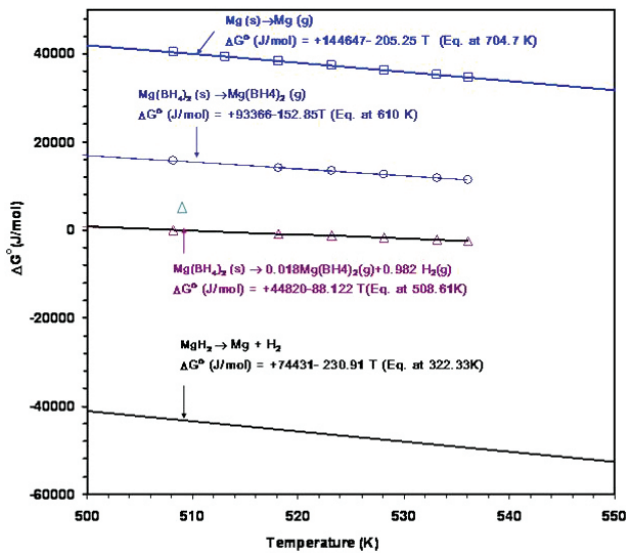
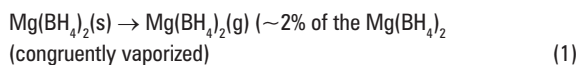


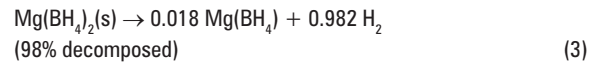
FIGURE 3. Gibbs energy (ΔG°) for the reactions for $\text{Mg}(\text{BH}_4)_2$ showing the two different pathways for the Li-N-H system.

(B) Thermodynamics of Vaporization of $\text{Mg}(\text{BH}_4)_2$

Contamination of a hydrogen storage system is also possible due to release of vapors from *the hydride compounds themselves*. In some cases the hydrides decompose and release elemental or molecular compounds during desorption processes in hydrating bed, especially under vacuum testing. This behavior of the complex hydride materials was evaluated by using a torsion effusion Knudsen cell method at UNR. In this method, we can obtain the vapor pressure as well as the molecular weight of the effusing species which yields the disproportionation aspects of the systems under consideration. The details of the experimental methods used were presented in the earlier reports. This report gives thermodynamic analyses of vaporization of $\text{Mg}(\text{BH}_4)_2$. Vapor pressures of $\text{Mg}(\text{s}) \rightarrow \text{Mg}(\text{g})$ and decomposition of $\text{MgH}_2 \rightarrow \text{Mg}(\text{s}) + \text{H}_2$ are included for comparison purposes. At 225°C , $P_{\text{H}_2} = 8.8 \times 10^{-6}$ atm, and $P_{\text{Mg}(\text{BH}_4)_2} = 2.03 \times 10^{-7}$ atm. There is no indication that Mg vaporization occurs (up to 233°C). There is some amount of expected $\text{Mg}(\text{BH}_4)_2$ ($\sim 2\%$) vaporized and the rest ($\sim 98\%$) is hydrogen, i.e. there is decomposition of the borohydride. Above 226°C (509 K) the ΔG° becomes negative and vigorous vaporization (hydrogen gas) starts. We propose two principal reactions for which the thermodynamic parameters are determined for magnesium borohydride, and presented in Figure 3:

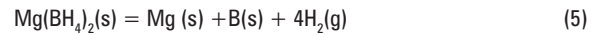


$$\text{Vapor pressure Eq.: } \log P(\text{bar}) = 2.216 - 4485/T, \text{ and } \Delta G^\circ(\text{J/mol}) = 93366 - 152.85 T \quad (\text{Eq. at } 610 \text{ K}) \quad (2)$$

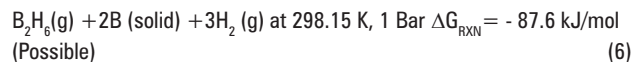


$$\text{Vapor Pressure Eq.: } \log P(\text{bar}) = 2.646 - 3871/T, \alpha \nu \delta \Delta G^\circ(\text{J/mol}) = 44280 - 88.122 T \quad (\text{Eq. at } 508.61 \text{ K}) \quad (4)$$

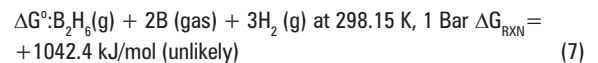
Above 235°C (508 K) the $\text{Mg}(\text{BH}_4)_2$ powder sample shows complete decomposition according to the reaction:



The presence of Mg metal in the residual sample was confirmed by XRD analyses. We did not observe Boron metal Bragg peaks in the XRD pattern, but it is most likely amorphous. Thus information from the torsion effusion experiments is useful to determine the stability of the borohydrides. There are always very valid questions regarding borane or other toxic gases evolving during decomposition of $\text{Mg}(\text{BH}_4)_2$. Using our data we calculated the average molecular weight (MW) of effusing gases which in this case the $\text{MW} = 2.42$ g/mol that suggests that the majority of the gas was hydrogen. Also, thermodynamic analyses revealed that B_2H_6 , if formed, may decompose to boron (metal) and hydrogen according to the equation:



However, boron *gas* formation is not likely from the decomposition of B_2H_6 , as the equation below shows positive:



To summarize, the vapor pressures of $\text{Mg}(\text{BH}_4)_2$ below 233°C are quite low and there hydrogen gas release. The vapor pressure of $P_{\text{Mg}(\text{BH}_4)_2} = 8.7 \times 10^{-7}$ bar and $P_{\text{H}_2} = 8.7 \times 10^{-7}$ bar at 255°C .

(C) Phase Transformations in $\text{Ca}(\text{BH}_4)_2$

Calcium borohydride studies were performed in collaboration with Ewa Ronnebro of Sandia National Laboratories and Yaroslav Filinchuk of ESRF, Grenoble, France using high resolution synchrotron SRD at ESRF. In this, we used commercial $\text{Ca}(\text{BH}_4)_2 \cdot 2$ -tetrahydrofuran from Aldrich corporation that was desolvated according to reference [8]. The crystal structure details, although determined, are left out in this report as the manuscript for publication is in reviews process. Other researchers, such as, Konoplev et al. [9], Miwa et al. [10], and Kim et al. [11] were also working on this problem around that time. A recent thermal-gravimetric study by Kim et al [11] indicated partial reversibility (90 bar) based on thermogravimetric results.

In situ XRD data showed that there were three phase transitions, $\alpha \rightarrow \alpha' \rightarrow \beta$ phases a small amount of β phase was present in the sample when we desolvated the tetrahydrofuran, so the samples were mixtures of α - and β -phases. Upon heating, the α -phase $\text{Ca}(\text{BH}_4)_2$ cell parameter a increased, whereas the c -parameter decreased up to phase transition to the tetragonal α' -phase at 222°C. In situ synchrotron diffraction data taken between 44–382°C show all the three $\text{Ca}(\text{BH}_4)_2$ phases in the expanded X-axis, 2θ scale, 10–22°, in the Figure 4. The changes in unit cell parameters and volume/ z of the unit cell, as a function of temperature, have been calculated from the data for the orthorhombic and tetragonal cells. The β -phase is 3.7–5.6% denser than the α - and α' -phases, depending on the temperature, the latter polymorphs transform into the stable β -phase in the temperature range of 177°C to 297°C. The unit cell parameters a and c (Å) and UC volume (Å^3) of the stable β - $\text{Ca}(\text{BH}_4)_2$ increase linearly with temperature (K): $a = 6.9187(1) + 2.821(7) \cdot 10^{-4}T$, $c = 4.34459(9) + 2.062(5) \cdot 10^{-4}T$, $V = 207.938(5) + 2.725(3) \cdot 10^{-2}T$. Further, β - $\text{Ca}(\text{BH}_4)_2$ completely decomposes between 382°C and 387°C. The phase transformations observed in the in situ synchrotron experiments are supported by thermogravimetric analysis (TGA) and difference scanning calorimetric experiments performed at the Sandia National Laboratories (not shown here). This study suggests that the decomposition products from a desolvated sample of $\text{Ca}(\text{BH}_4)_2$ and a solid-state prepared catalyzed sample of $\text{Ca}(\text{BH}_4)_2$ may be different from the high pressure synthesized sample.

Conclusions

1. Imide-Amide (Li_2NH - LiNH_2) Impurity Effects (UNR Sample):
 - Studies on trace amounts of impurity gases (100 ppm) such as O_2 , CO , H_2O , and CH_4 , in H_2 and industrial hydrogen, up to ~1,100 cycles showed that the O_2 impurity was most

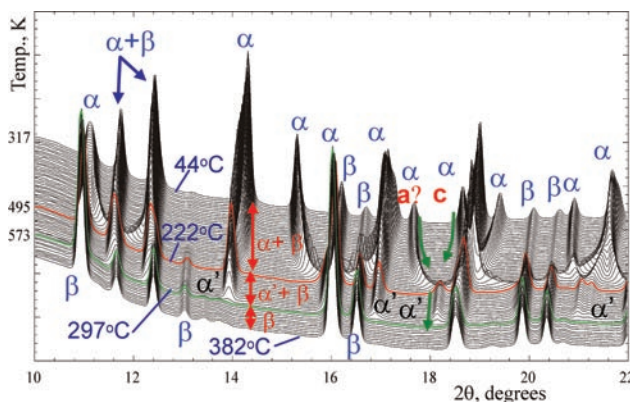


FIGURE 4. In situ synchrotron XRD at different temperatures show phase transformations, from $\alpha \rightarrow \alpha' \rightarrow \beta$ phase.

detrimental to the cycling behavior of amide-imide hydrides. The H_2O (100 ppm) impurity surprisingly showed lower loss as compared with oxygen (100 ppm) impurity.

- Carbon monoxide was the least reactive and did not show significant loss in capacity.
 - Cycling with methane showed a little loss in hydrogen capacity. Aging results also showed no significant loss in capacity.
2. Vapor Pressure Measurement of $\text{Mg}(\text{BH}_4)_2$ (Sample from GE):
 - No significant vaporization of $\text{Mg}(\text{BH}_4)_2$. Below 233°C it is not possible to record any vapor pressure data. However, above 233°C the ΔG° becomes negative and vaporization starts. The ΔG° of $\text{Mg}(\text{BH}_4)_2$ was determined. $\text{Mg}(\text{BH}_4)_2 (\text{s}) \rightarrow \text{Mg}(\text{BH}_4)_2 (\text{g})$ ($\Delta H = 93.4 \text{ kJ/mol}$) (only ~2% of the vaporization). The majority of the vaporization was due to disproportionation of $\text{Mg}(\text{BH}_4)_2 \rightarrow \text{Mg}(\text{s}) + \text{B}(\text{s}) + 4\text{H}_2(\text{g})$, $\Delta H = 44.82 \text{ kJ/mol}$ (~98% majority hydrogen).
 3. Structure and Phase Transformations in $\text{Ca}(\text{BH}_4)_2$ (UNR-SNL Sample):
 - In situ synchrotron data showed two polymorphs of α - $\text{Ca}(\text{BH}_4)_2$ and a small amount of β -phase. A second order $\alpha \rightarrow \alpha'$ phase transition occurred at 222°C (confirmed by differential scanning calorimetry). Another phase transition, $\alpha' \rightarrow \beta$ phase upon heating above 297°C and decomposes at 382°C into unknown products which according to TGA is associated with a weight loss, likely due to release of hydrogen.

Future Directions

1. Continue Work on Effect of Impurities on Specific Contaminants: (a) Pressure cycling on mixed -Li based complex hydrides, (b) testing of hydrides developed by MHCoe partners.
2. Vapor Pressure Studies on LiBH_4 and other Borohydrides: Thermodynamics of vaporization of LiBH_4 and others.
3. Phase Diagram Determination of Mixed Complex Hydrides and CALPAHD Modeling; Initiate experimental development of non-equilibrium/equilibrium phase diagrams.
4. High Pressure Differential Scanning Calorimetric Research: Dynamic heating behavior of complex hydrides.
5. Lattice Dynamics of Imide-amides (a) Hydrogen Lattice Dynamics Studies on Complex Hydrides, University of Rome – International Energy Agency/ International Partnership for the Hydrogen

- Economy (IEA/IPHE) Proposal, “Hydrogen Dynamics, Lattice interactions, and Atomic-scale Structure of Complex/Chemical Hydrides”.
6. Effect of Solid State impurities in complex Hydrides and Phase Equilibria: (a) Collaboration between Cantelli (Rome, Italy) and Chandra-Jensen, (USA), (b) IEA/IPHE Collaborative Studies at University of Geneva and CRNS (France) on defect structure thermodynamics and crystallography. Collaborative program between Chandra (USA)-Yvon (Switzerland)-Latroche (France).

FY 2008 Publications/Presentations

1. Wen-Ming Chien, Joshua Lamb, Dhanesh Chandra, Ashfia Huq, James Richardson Jr. and Evan Maxey, “Phase evolution of Li_2ND , LiD and LiND_2 in hydriding/dehydriding of Li_3N ,” *Journal of Alloys and Compounds*, Volumes 446-447, Pages 363-367, 31 October (2007).
2. A. Huq, J.W. Richardson Jr., E. Maxey, D. Chandra, W. Chien, “Structural Studies of Li_3N Using Neutron Powder Diffraction,” *Journal of Alloys and Compounds*, 436, pp. 256-260 (2007).
3. A. Huq, J.W. Richardson Jr., E. Maxey, D. Chandra, W. Chien, “Structural Studies of Deuteration and De-deuteration of Li_3N by Use of In Situ Neutron Diffraction,” *Journal of Physical Chemistry C*, 111 (28), pp. 10712-10717 (2007).
4. W. Chien, J. Lamb and D. Chandra, “Structural Behavior and Pressure Cycling Effect Studies of Li-Based Complex Hydrides,” *TMS2007 Extraction, Processing, Structure and Properties Proceedings, General Abstracts: Structure Materials Division*, pp. 143-149 (2007).
5. Dhanesh Chandra, Part III - Metal Hydrides, AB_3/AB Intermetallics for Hydrogen Storage, Gavin Walker, editor, Woodhead Publishing, UK, in Print (submitted 2007).
6. W. Chien, D. Chandra, J.H. Lamb, “X-ray Diffraction Studies of Li-Based Complex Hydrides after Pressure Cycling,” *Advances in X-ray Analysis*, vol. 51 (2007)-accepted manuscript – in print.
7. Lithium Nitride as Hydrogen Storage Material, O. Palumbo, A. Paolone, R. Cantelli, and D. Chandra, HYSYDAYS – PROCEEDING, 2nd WORLD CONGRESS OF YOUNG SCIENTISTS ON HYDROGEN ENERGY SYSTEMS, – Turin, Italy, 2007, 1-4. (IEA Collaboration), (2007)
8. Dhanesh Chandra, Joshua Lamb, Raja Chellappa, Wen-Ming Chien, “Effect of Gaseous Impurities on Long-Term Thermal Cycling/Aging Properties of Complex Hydrides for Hydrogen Storage” DOE - Sandia National Laboratory Program Review Meeting, December 10th and 11th, 2007, Livermore, CA.
9. D. Chandra, *Extrinsic Effects of Impurities on Long-Term Behavior of Complex Hydrides, Task 22 - H18, International Energy Agency Task 22 and Task 19 – Workshop St-Alexis-des-Monts, Québec, Canada, Hotel Sacacombe: March 1st to 5th*, 2008 Organizers: B. Hauback (Norway), R. Chahine, and N. Beck (Canada).

References

1. G. Burkhordarian, T. Klassen, M. Dornheima, R. Bormann, J. of Alloys and Compounds, 2007, 440, 18.
2. P. Chen, Z. Xiong, J. Luo, J. Lin, and K. Tan, *Nature* 21 (2002) 302.
3. A. Rabenau and H. Schultz, *J. Less Common Metals*, 50 (1976), 155-159. Also see, D.H Gregerery, P:M.O'mera, A.G. Gordon, J.P. Hodges, S. Short, and J.D. Jorgensen. *Chem. Mater.*, 14 (2202), 2063-2070. Li_3N .
4. K.Weidner, E., D.K. Ross, et al. *Chemical Physics Letters*, 2007. 444(1-3): p. 76-79.
5. R. Niewa and D.A. Zhrebtsov, *Z. Kristallogr.* NCS 217 (2002) 317–318.
6. T. Noritake, Orimo, et al. *J. Alloys Compds.* 393 (2005), 264-268.
7. K. Miwa, N. Ohba, S. Towata, Y. Nakamori, and S. Orimo *Physical Review*, B71(2005), 195109.
8. V.N. Konoplev, Sizareva, A.S., *Koord. Khim.* 1952, 18, 508.
9. K. Miwa, K.; Aoki, K.; Noritake, T.; Ohba, N.; Nakamori, Y.; Towata, S.; Züttel, A.; Orimo, S., *Phys. Rev. B*, 2006, 74, 155122.
10. S.A. Kim, S-A. Jin, J-H. Shim, Y.W. Cho, *Scripta Materialia*, in press.